Article

Journal of
Nanoscience and Nanotechnology
Vol. 18, 6650–6652, 2018
www.aspbs.com/jnn

Electronic Structures of Strained $InAs_xP_{1-x}$ by Density Functional Theory

Seung Mi Lee*, Min-Young Kim, and Young Heon Kim

Korea Research Institute of Standards and Science (KRISS), Daejeon 34113, Korea

We investigated the effects of strain on the electronic structures of $InAs_xP_{1-x}$ using quantum mechanical density functional theory calculations. The electronic band gap and electron effective mass decreased with the increase of the uniaxial tensile strain along the [0001] direction of wurtzite $InAs_{0.75}P_{0.25}$. Therefore, faster electron movements are expected. These theoretical results are in good agreement with the experimental measurements of $InAs_{0.75}P_{0.25}$ nanowire.

Keywords: Density Functional Theory, Group III–V, Nanowire, Strain.

1. INTRODUCTION

Density functional theory (DFT) is a quantum mechanical simulation method which, over the past decades, has been successfully employed to reveal atomic and electronic properties of many-body systems such as semiconductors, surfaces, and nanostructures.[1,2] Strain-induced modifications of electronic and vibration properties of materials including silicon (Si),[3] indium arsenide (InAs),[4] and alumina (Al_2O_3)[5] have been studied both experimentally and theoretically in the field of device properties enginnering.

Group III–V materials, such as InAs, $InAs_xP_{1-x}$, and InP, have attracted significant attention owing to their potentials for applications in electric and optoelectric devices.[6] Strain effects on the electrical and piezoelectric properties of InAs nanowires have been experimentally studied.[7,8] Recently, results of *in-situ* measurements of electromechanical properties of $InAs_xP_{1-x}$ nanowires suggested that the change of the carriers' mobilities emerge owing to the mechanical tensile strain along the axis direction of the nanowires.[9] High-resolution transmission electron microscopy showed that the studied nanowires consist of a mixture of wurtzite and zincblende structures; the nanowire's axial direction was along the [0001] direction of wurtzite $InAs_xP_{1-x}$. Experimental observations showed that the content of P in $InAs_xP_{1-x}$ nanowire was ~25%.[9]

In this report, we theoretically investigate the electronic structure of $InAs_{0.75}P_{0.25}$ under uniaxial strain along the [0001] direction of the wurtzite structure. By performing DFT calculations, we showed that the effective mass of the electrons decreases with the increase in the uniaxial tensile strain; therefore, faster movements of electrons are expected. It was obtained that the electron's effective mass increases with the compressive uniaxial strain. Our theoretical findings are in agreement with the experimental observations reported for $InAs_{0.75}P_{0.25}$ nanowires.

2. CALCULATION DETAILS

We performed quantum mechanical DFT calculations. Atomic orbital basis sets were used, as implemented in DMOL3 code,[10] by employing double numerical set with polarization and diffusion function forms. All electrons, including those of the cores, were considered in the calculations. Exchange-correlation functional obtained using local density approximation (LDA) and Monkhorst-Pack grid points (separation of 0.015 $Å^{-1}$) were employed. The employed geometry optimization criteria for distance, force, and total energy were 0.005 Å, 0.001 Ha/Å, and 10^{-5} Ha, respectively.

In quantum mechanical calculations, it is always preferred to simplify the complex real system, as it is almost impossible to model the whole system using its real size. For example, experimental results, which motivated us to perform this study, showed that the studied nanowire had a diameter of 110 nm and contained a mixture of wurtzite and zincblende structures including dislocations. Such system cannot be effectively modeled using proposed calculation methods, as they are suitable for systems that have

*Author to whom correspondence should be addressed.

 1533-4880/2018/18/6650/003 doi:10.1166/jnn.2018.15712

less than one thousand atoms. Therefore, for the calculations, we considered the wurtite $InAs_xP_{1-x}$ structures with a fixed composition of As and P, known from the experiements ($InAs_{0.75}P_{0.25}$).[9]

The carrier mobilities were calculated using the band structure and Eq. (1).[11]

$$\frac{1}{m^*} = \frac{1}{\hbar^2} \cdot \frac{d^2\varepsilon}{d\kappa^2} \quad (1)$$

We calculated the second derivatives of the bands in the E–K plot using numerical interpolation assuming parabolic shape near the minima of the conduction band and maxima of the valence band for the holes and electrons, respectively.

3. RESULTS AND DISCUSSION

As benchmark calculations, we performed calculations for the bulk InAs using different basis sets and exchange-correlation functionals. For zinc blende InAs, LDA calcualtions showed that the lattice constant is $a = 6.0862$ Å and the electronic band gap is 0.388 eV, while the generalized-gradient-approximation (GGA) calculations using Perdew–Burke–Ernzerhof (PBE) functional[12] showed that $a = 6.2369$ Å and that the band gap is 0.244 eV. Compared with the experimental values of the lattice constant ($a = 6.0583$ Å) and electronic band gap (0.35 eV),[13] LDA results showed better agreement. Therefore, we employed the LDA functional for the calculations. Similarly, for the wurtzite InAs, the calculated values of the lattice constants using LDA ($a = 4.2940$ Å and $c = 7.0632$ Å) were in a better agreement with the experimental values, compared with those obtained using GGA-PBE ($a = 4.4028$ Å and $c = 7.2333$ Å); the same trend was observed for the band gap (0.406 eV by LDA and 0.264 eV by GGA-PBE). Using the optimized bulk InAs structure, we generated a supercell ($1 \times 1 \times 2$ repeating unit), substituted an arsenic (As) atom with a phosphorus (P) atom,

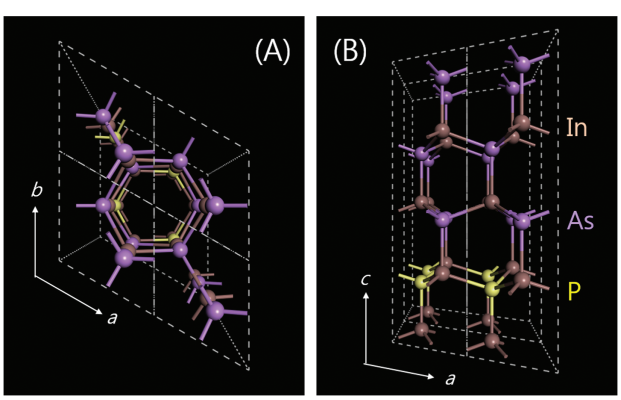

Figure 1. Optimized atomic structure of $InAs_{0.75}P_{0.25}$ shown as a ball-and-stick model: (a) Top and (b) side view. Dashed lines outline the primitive cell, while the white arrows represent the lattice vectors. The brown, purple, and yellow balls represent indium, arsenic, and phosphorus atoms, respectively.

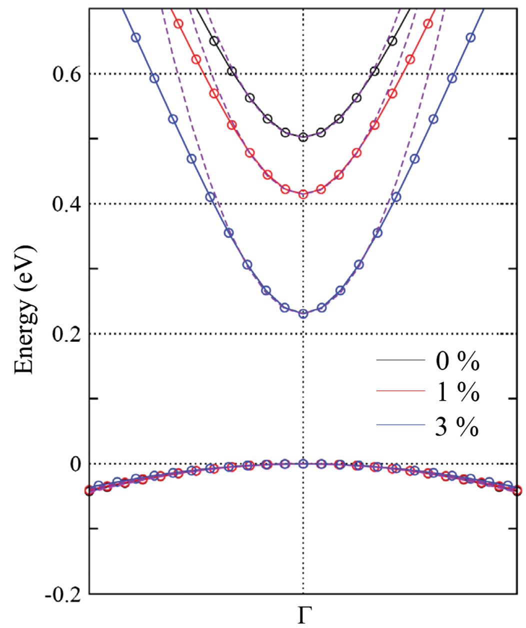

Figure 2. Calculated electronic band structures for the lowest conduction band (CB) and highest valence band (VB) near the Gamma-point under tensile strains. The black, red, and blue curves represent the bands of the structures under tensile strains of 0%, 1%, and 3%, respectively. The dashed violet curves represent the fitting, which can be employed to obtain the second derivatives near the top of the VB and bottom of the CB, in order to reveal the effective masses of the carriers using Eq. (1).

and then fully relaxed the supercell. The optimized atomic structure of $InAs_{0.75}P_{0.25}$ is shown in Figure 1 as a ball-and-stick model along different viewing directions. The dashed lines outline the primitive cell, while the white arrows represent the lattice vectors. The brown, purple, and yellow balls represent In, As, and P atoms, respectively.

On the optimized $InAs_{0.75}P_{0.25}$ structure, we applied uniaxial tensile strain along the [0001] direction by reducing the supercell size along this direction by 1% and 3%. After internal relaxation, i.e., ion relaxations without optimizing the cell parameters, electronic band structure calculations were performed on the optimized structure. The calculated electronic band structures with conduction band minimum and valence band maximum under tensile strains near the Gamma-point are shown in Figure 2. The black, red, and blue curves correspond to tensile strains of 0%, 1%, and 3%, respectively. It can be noticed that with the increase of the tensile strain, the lowest conduction band

Table I. DFT calculation results of wurtzite $InAs_{0.75}P_{0.25}$ under uniaxial tensile strain along the [0001] direction. E_{gap} is the electronic band gap, m_e^* is the effective mass of the electron, and m_0 is the free-electron mass. The effective masses of the carriers are in units of m_0.

Tensile strain (%)	a (Å)	$2c$ (Å)	E_{gap} (eV)	m_e^*/m_0
0	4.2582	14.0171	0.502	0.0250
1	4.2582	14.1573	0.414	0.0233
3	4.2582	14.4376	0.231	0.0211

Table II. DFT calculation results of wurtzite $InAs_{0.75}P_{0.25}$ under uniaxial compressive strain along the [0001] direction.

Compressive strain (%)	a (Å)	$2c$ (Å)	E_{gap} (eV)	m_e^*/m_0
0	4.2582	14.0171	0.502	0.0250
1	4.2582	13.8769	0.586	0.0358
3	4.2582	13.5966	0.714	0.0484

becomes sharper at the Gamma-point, while the highest valence band does not change significantly. The violet dashed curves represent the fitting, which can be employed to obtain the effective masses of the carriers. The carriers' mobilities were obtained using the band structures by employing the approach discussed above. The sharper band shape implies smaller effective mass (Eq. (1)). The calculation results are summarized in Table I. It can be noticed that the electron effective mass m_e^* decreases with the increase of the uniaxial tensile strain. We considered only the electron carriers, as it was obtained that the hole effective mass (0.539 m_0 for a strain-free system) is significantly larger than that of the electron, hence the holes would not significantly contribute to the transport properties, compared with the electrons. These theoretical results suggest that the electrons move faster when a tensile strain is applied to the $InAs_{0.75}P_{0.25}$ nanowire along the axial direction during the electromechanical experiments, compared with the strain-free structure. These findings could be employed for fast and accurate measurements.

In addition, we performed calculations for uniaxial-compressive-strained $InAs_{0.75}P_{0.25}$ along the [0001] direction by 1% and 3%, using the same methods. Under compressive strain, we obtained that the electron effective mass m_e^* decreases with the increase of the strain, which is not desirable for fast *in-situ* measurements. The calculation results are listed in Table II.

4. CONCLUSION

We performed quantum mechanical DFT calculations to reveal the effects of tensile strain on the effective masses of the charges in $InAs_{0.75}P_{0.25}$, motivated by experimental results from precise measurements.[9] The calculations showed that the effective mass of the electrons decreased with the increase of the uniaxial tensile strain, which is consistent with the experimental findings. For the strain-free, 1%-strained, and 3%-strained structures we obtained effective masses of 0.0250 m_0, 0.0233 m_0, and 0.0211 m_0, respectively, where m_0 is the free-electron mass. The obtained theoretical results were in good agreement with the experimental observations.

Acknowledgments: This research was supported by Nano-Materials Technology Development Program of the NRF of Korea funded by MEST (NRF-2016M3A7 B4025406).

References and Notes

1. J. Neugenbauer and T. Hickel, *WIREs Comput. Mol. Sci.* 3, 438 (**2013**).
2. M. Bockstedte, A. Kley, J. Neugenbauer, and M. Scheffler, *Comput. Phys. Comm.* 107, 187 (**1997**).
3. Y. S. Kim and S. M. Lee, *Phys. Rev. B* 75, 165304 (**2007**).
4. T. Hammerschmidt, P. Kratzer, and M. Scheffler, *Phys. Rev. B* 75, 235328 (**2007**).
5. S. M. Lee, N. Kim, I. Y. Jung, C. S. Kim, and H. Yu, *J. Nanosci. Nanotechnol.* 17, 8378 (**2017**).
6. V. Swaminathan and A. T. Macrander, Materials Aspects of GaAs and InP Based Structures, Prentice-Hall, Inc., USA (**1991**).
7. K. Zhang, Z. Zhang, Y. Hu, P. Chen, W. Lu, J. Drennan, X. Han, and J. Zou, *Nano Lett.* 16, 1787 (**2016**).
8. X. Li, X. Wei, T. Xu, D. Pan, J. Zhao, and Q. Chen, *Adv. Mater.* 27, 2852 (**2015**).
9. J. H. Lee, M. W. Pin, S. J. Choi, M. H. Jo, J. C. Shin, S.-G. Hong, S. M. Lee, B. Cho, S. J. Ahn, N. W. Song, S.-H. Yi, and Y. H. Kim, *Nano Lett.* 16, 6738 (**2016**).
10. B. Delly, *J. Chem. Phys.* 113, 7756 (**2000**), As implemented in Dassault Systems Biovia Corp.
11. C. Kittel, Introduction to Solid State Physics, John Wiley & Sons, Inc., New York (**1986**).
12. J. P. Perdew, K. Burke, and M. Ernzerhof, *Phys. Rev. Lett.* 77, 3865 (**1996**).
13. D. R. Lide, Handbook of Chemistry and Physics, 84th edn., CRC Press, Boca Raton, USA (**2003**).

Received: 4 August 2017. Accepted: 22 November 2017.